

Improved Hydrographic Surveying Accuracy with the Use of GPS/IMU and Single Beam Echo Sounder

Van Dinh Hoang, Nguyen Ngoc Quynh, Ha Manh Tuan*

School of Transportation Engineering, Hanoi University of Science and Technology, Hanoi, Vietnam

*Email: tuan.hamanh@hust.edu.vn

Abstract

Single beam echo sounders (SBES) mounted on unmanned surface vehicles (USVs) are widely used in hydrographic surveying, particularly for detecting water depth and digital depth mapping, among other things. Because of conditions such as ocean waves, the relative level arm of each component, and errors in each component device, using only SBES and GPS sensors leads to significant errors and poor accuracy. Now the SBES sensor's accuracy has improved. However, this is insufficient. A new real-time kinematic (RTK) positioning technique enables horizontal and vertical coordinate precision of 2 to 5 centimeters. Additionally, the precision of the survey is dependent on the USV's movements. USVs use inertial measurement units (IMUs) to provide information on the system's acceleration, velocity, position, and orientation. To reduce errors and produce trustworthy results, it is necessary to process data from various devices using a well-integrated algorithm. The purpose of this article is to discuss how to develop an algorithm that combines sensors such as GPS RTK/IMU, SBES, and other similar devices. This method takes into account both the rotations and relative level-arm of sensors. Finally, analysis of the data indicates a significant increase in the accuracy of the integrated algorithm when compared to the conventional techniques.

Keywords: GNSS RTK, IMU, level arm, single beam echo sounder.

1. Introduction

Depth surveying is critical for monitoring the quality of waterway flow and for forecasting the quantity of sedimentation in river and lake environments. Underwater topographic measurement is primarily concerned with the coordinates and depth of the measuring spot by using classic methods such as optical instruments, depth poles, and total station methods to calculate the longitude and latitude of the measuring site [1]. With the advancement of navigation technology, utilizing GPS to establish the coordinates of the depth measuring site increases productivity, provides rapid results, and shortens survey time. However, typical GPS devices have a considerable position error of 40-50 cm, reducing the dependability of survey data and resulting in low efficiency. It delivers a new identification method based on the reference data determined by the base station by utilizing real-time kinematic (RTK) GPS positioning technology.

RTK stands for Real Time Kinematic, and is a method of real-time kinematics positioning, which is a sophisticated technique that eliminates errors and improves accuracy to the maximum when positioning GNSS satellites. The RTK concept is shown in Fig. 1. To measure RTK, up to 2 dedicated GNSS receivers are required: one located at a fixed location (called the base station), and one mobile device at the points to be

measured (called the Rover Station). The base station is responsible for receiving signals from many satellites at the same time, in many different frequency bands to ensure accuracy, and then transmitting the corrected signal to the Rover station.

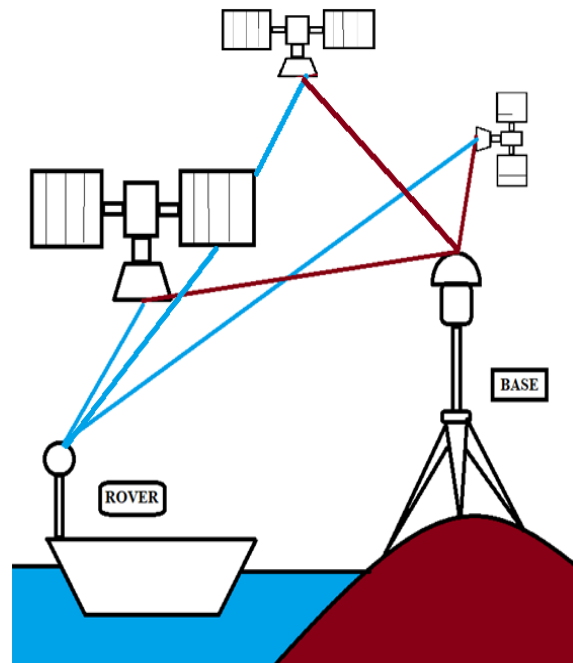


Fig. 1. RTK concept

The Rover station, in addition to receiving satellite signals like the base station, also has to receive the correction signal from the base station, then compare and calculate it to give the most accurate results for the measurement.

This project uses the RTK measurement method using the CORS station. A CORS station (Continuous Operation Reference Station) is a system of stations that continuously monitor and receive GNSS signals at fixed points, give a quick position, and then transmit that data through the Internet to form a network. In the RTK measurement method, the CORS station acts as a Base station, and the user only needs to connect the mobile station to the CORS station to be able to measure the RTK. Using the CORS station in RTK measurement has many advantages, such as: wide coverage (currently covering all provinces in Vietnam), completely free, stable signal, and guaranteed accuracy.

To detect the depth of water, more complex echo sounding technology employs two forms of echo sounding: single-beam echo and multi-beam echo [2]. An echo sounder uses the following principle: a projector generates sound waves, and a receiver, or hydrophone, receives the echo. If the transmitter is able to both produce and receive sound waves, it is referred to as a transducer. Based on the travel time or the energy of the reflected waves, the respective depth or bottom type can be assessed. Obviously, the results depend upon the emitted frequencies. Low frequencies are less absorbed and are thus able to reach further than high frequencies.

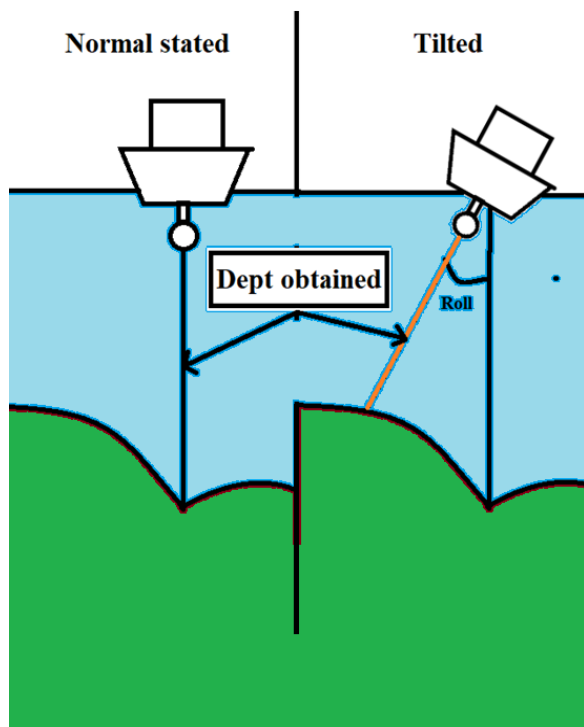


Fig. 2. Depth obtained in the normal state and when tilted

This is why low frequencies can be used to monitor a large area, but with a lower resolution (low quality). A single-beam sonar emits one vertical acoustic pulse (ping). The transducer receives a part of the echo and, thus, the depth can be calculated by using the travel time of the pulse. The single-beam can be a dual-beam. This means that the sonar can emit both a high-frequency pulse and a low-frequency pulse at the same time. As a result, better detection of the softer sediments can be achieved, and mobile mud layers can be detected. Measurement results obtained from GPS and ultrasonic sensors are affected by the state angles of the system. The accuracy of the measurement point location depends on the ability to compensate for position errors caused by the roll, pitch, and yaw angles of the survey vessel. In deep water situations, even a tiny tilt angle can result in significant mistakes. Fig. 2 shows the error when the survey boat is tilted. Therefore, it is necessary to install inertial measurement units (IMUs) to determine the state angles of the system.

Numerous articles have been published on the subject of depth determination using ultrasonic technology. Analyzed and summarized the sources of error and corrective procedures for multi-beam sound depth measurement, as well as comparing the data under various variables such as sound speed, depth, and GPS accuracy. The document [3] compares the accuracy of standard GPS data to that of RTK GPS data. The document [4] illustrates the relationship between high-resolution side-scan sonar images and seafloor topography and provides a new way of recovering the bottom depth more accurately. However, the model is somewhat complex and complicated. The article [5] described how a topographic survey was conducted using the single-beam echo sounding (SBES) method and how a basic measurement method was devised to suit the technical requirements. Today, the primary method of estimating underwater depth is using single-beam or multi-beam depth measurement equipment. While a multi-beam echo sounding system can capture hundreds of depth points in a single measurement, providing high resolution, multi-beam depth sensors are frequently affected by the sound velocity and angle of the beam, necessitating the use of expensive and highly accurate position and state compensators. While it is possible to conduct surveys in shallow water and coastal areas using LIDAR technology, data processing remains extremely challenging, and the resulting products are often insufficient and rarely used [6]. Echo sounding is a highly effective method for determining underwater depths that may be used in both huge areas and deep bodies of water. Single-beam echo sounding sensors with the lowest cost are commonly used to determine the distance between the point of sound creation and the surface of underwater terrain. They are widely used to measure inland deep channels, dams, canals, and lakes.

This paper discussed how to detect the underwater terrain by merging a GPS/IMU depth measuring system and a single-beam echo sounding instrument. To validate the algorithm, create a data model in Mat Lab/Simulink that includes models for GPS, IMU, and ultrasonic sensors. This paper describes a method for developing an underwater depth measuring system using a combination of three types of sensors, including an IMU, a GPS RTK, and an acoustic wave sensor. The approach's results contribute to an increase in survey quality when compared to conventional methods.

2. System Design

The integrated system shown in Fig. 3, consisting of an embedded computer, will collect data from the ultrasonic Ping sonar sensor, the RTK GPS receiver, and the IMU system.

Ping sonar is a device that uses sound in order to identify objects in the water column. It's known as a "SONAR" system (Sound Navigation and Ranging). Active sonars produce their own specific sound waves and analyze the reflection (echo) of the emitted waves (echo sounder). Active sonars include multi-beam and single-beam sonars. A single-beam sonar is used to make bathymetric maps as well as to investigate fish

populations and dynamics. This single-beam acoustic depth sensor has a range of 0.5 m to 50 m and a beam width of 30 degrees. The transducers transmit at 115 kHz and the resolution ranges from 25 cm to 1 cm at 50 m and 2 m, respectively. These are technical parameters for surveying the depth of river channels and lakes. And specifically, the project will use the PING-SONAR-R2-RP sensor.

The Inertial Measurement Unit (IMU) is a specialized device that measures the angle of rotation and inclination of systems (IMU-containing systems), such as boats, aircraft, or equipment that requires balance. The IMU sensor is comprised of three internal sensors: an accelerometer, a gyroscope, and a magnetometer. A full IMU module would be called 6-DOF (6 Degrees of Freedom), i.e., 6 independent axes (3 of acceleration and 3 of gyro). Sometimes that's not enough though; more complex projects such as navigating aircraft or robotics may require a 9-DOF (additional 3-axis magnetic field sensor-magnetometer) that acts almost like a compass for orientation), or 10-DOF (adds a barometer-used to measure altitude), or even 11-DOF (adds a GPS module to determine position). However, most home-made applications require only a 6-DOF IMU.

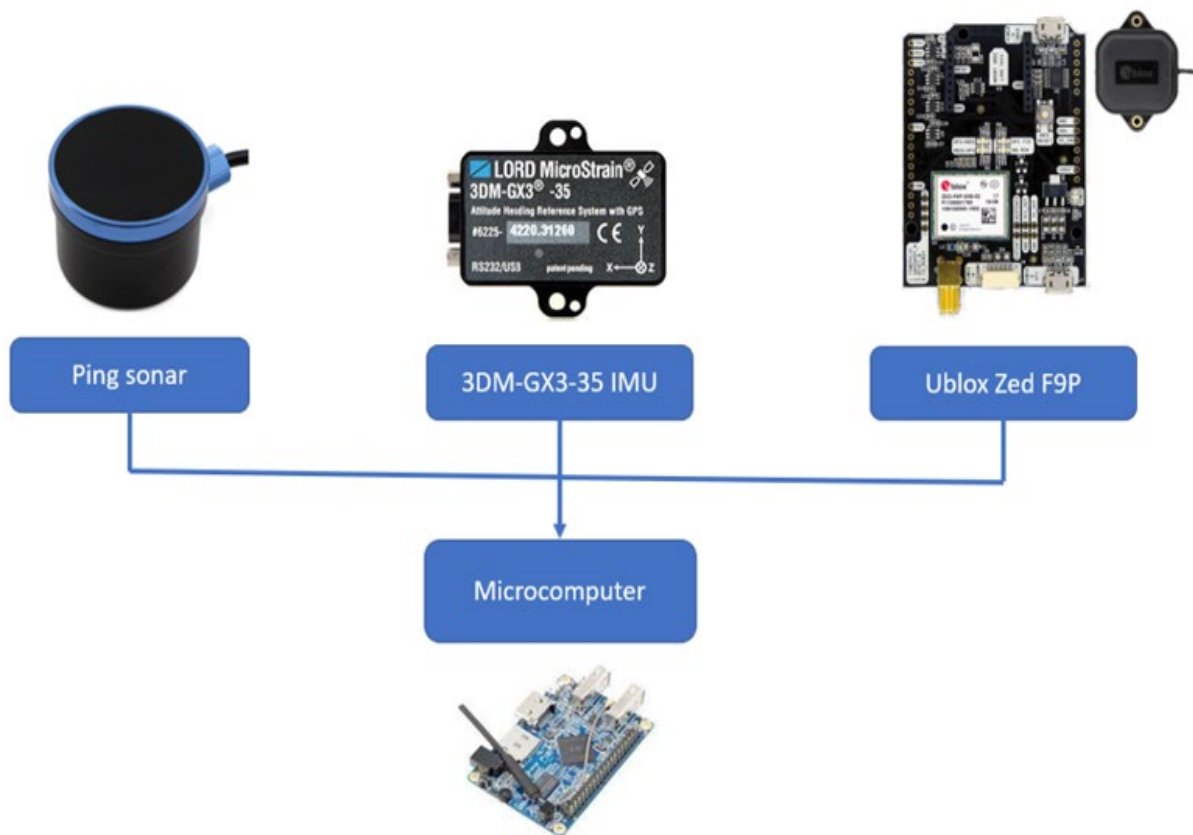


Fig. 3. The hardware GPS/IMU and SBES system

The IMU sensor will determine the device's tilt angle in relation to a preset plane, from which the device can be rebalanced on the plane by computing the change in acceleration or rotation in relation to the plane. The device's state (roll, pitch, and yaw) and heading are determined using an IMU LORD Micro Strain 3DM-GX3-35 system. The IMU 3DM-GX3-35 includes a built-in GPS module, but its location accuracy is limited, so it is recommended to utilize an external GPS in addition to RTK technology capable of centimeter-level positioning. The U-blox ZED-F9D receiver is a dual-frequency device capable of receiving signals from four location systems: GPS (L1C/A, L2C), GLONASS (L1OF, L2OF), Galileo (E1B/C, E5b), and BeiDou (B11, B21). In good satellite signal conditions and with no obstructions around the antenna frame, the receiver will provide timely position results by utilizing RTK technology for precision (1 cm + 1 ppm). The gadget operates in temperatures ranging from -40 °C to 85 °C and features a large number of physical communication connectors. The programming libraries, device settings, and setup instructions are all provided in whole by the manufacturer, and information about them is readily available.

An embedded computer is a device or a system designed with the purpose of serving a certain requirement, problem, or function. Embedded computers are widely applied in the fields of industry, monitoring, communication, and control automation. The design of this computer is quite small compared to other general-purpose computers. On the other hand, its compact size makes it easy for large-scale or long-distance deployment. Embedded computers operate in harsh environments. In harsh environments, embedded PCs require a compact and rugged metal enclosure that uses fewer cables and no moving parts, such as hard drives and cooling fans. In addition, vibration and shock resistance can enhance the stability of systems used on buses, trucks, trains, and moving objects. The computer is designed to perform in extreme outdoor circumstances with temperatures ranging from -35 °C to +70 °C. An embedded computer running Linux and a real-time application for GPS, Ping sonar, and IMU data collection. Over time, the collected data will be synchronized. The hardware operation is represented in the picture, which depicts the mechanism by which each sensor communicates with and connects to the system.

3. Method

Underwater topographic survey is determined by two primary factors: the coordinates of the point to be surveyed and the underwater depth of the point. To obtain these values, rotations and axis transformations such as GPS, IMU, and ultrasonic axes are used. The GPS data is in the WGS84 coordinate system, and the received packets are in NMEA format, which contains

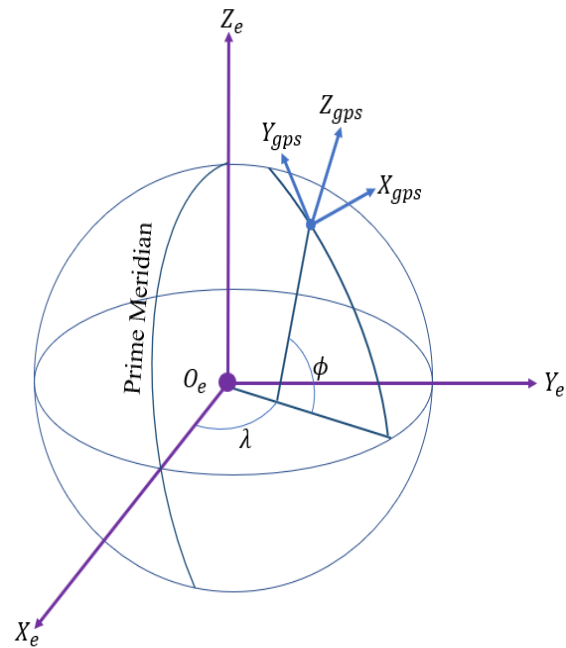


Fig. 4. ECEF and GPS coordinate systems

information about latitude ϕ , longitude λ , and height above the leveling plane (height in the WGS84 coordinate system). Fig. 4 shows the ECEF and GPS coordinate systems. To calculate, we convert the LLH tetrahedral coordinate to the ECEF by using documents [7]. Because the received data for ultrasonic sensors is the distance between the sensor and the bottom surface, the matrix $d(t)_p^{sbcs}$ is regarded as the position of the bottom point in the ultrasonic sensor's coordinate system. The IMU device will return a rotation matrix that will be used to convert the body's IMU coordinate system to the ENU coordinate system with the IMU origin, as well as the points in the body's IMU coordinate system that will be calculated and returned with the IMU origin value.

Assuming the equipment is permanently attached to the ship, the coordinate systems are configured as illustrated. To acquire an accurate result, it is critical to identify the relative level arm positions between the coordinate systems. The coordinates of each underwater location are obtained using (1), and Fig. 5 illustrates them in vector form [8].

The components of (1) are calculated by processing sensor data; for arm levels, the estimated deviation angle of the IMU, echo sounder, and GPS are computed during calibration using a direct measurement method. In comparison to commercially available systems, which provide only final findings, the test system has the advantage of collecting raw data, which allows for calibration. Calibration is a critical step because it minimizes the error variables between reference systems, hence minimizes the difference between the actual surface and the system's output.

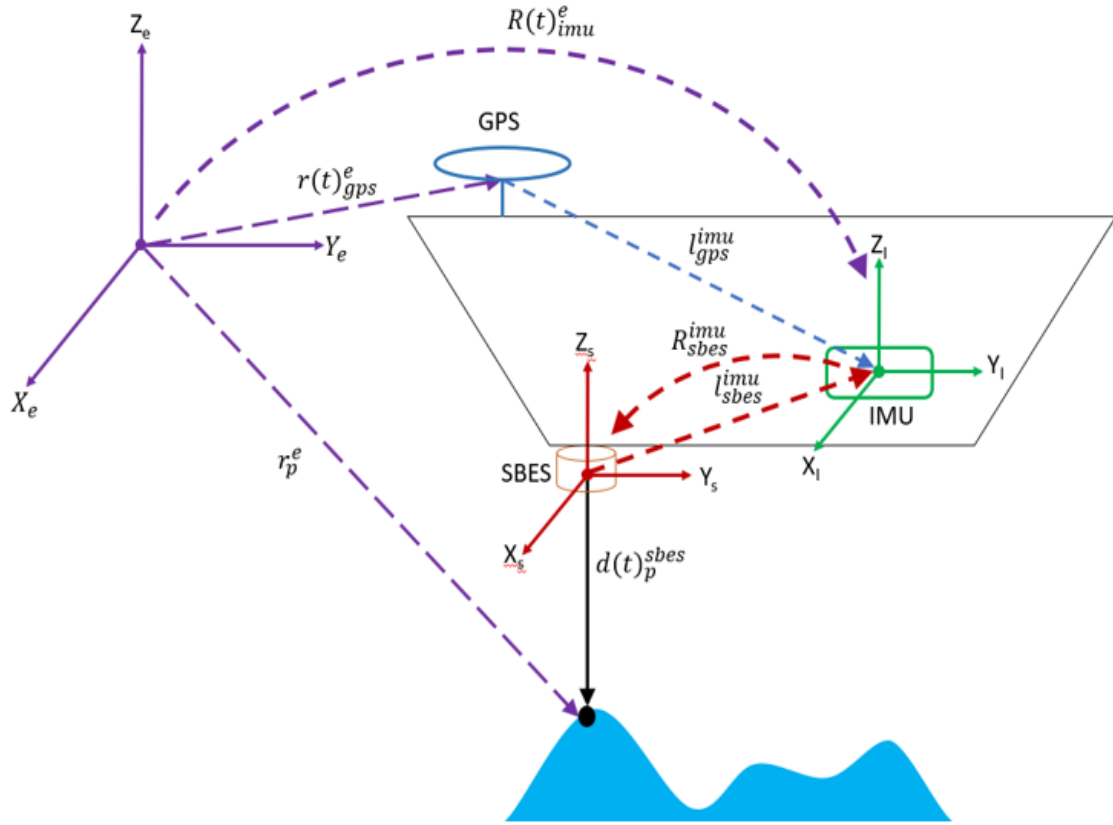


Fig. 5. Vectors' relative positions

$$r_p^e = r(t)_{gps}^e + R(t)_{imu}^e [l_{sbes}^{imu} - l_{gps}^{imu} - d(t)_p^{sbes} R_{sbes}^{imu}] \quad (1)$$

where:

r_p^e : position vector of the object point in the surveying coordinate system e

$r(t)_{gps}^e$: position vector of the GPS antenna in the coordinates system

$R(t)_{imu}^e$: rotation matrix between the IMU frame and the surveying coordinate system at time t

l_{sbes}^{imu} : position vector of the SBES in the IMU coordinate system

l_{gps}^{imu} : position vector of the GPS antenna in the IMU coordinate system

R_{sbes}^{imu} : rotation matrix between the SBES local coordinate system and the IMU coordinate system

$d(t)_p^{sbes}$: distance between the SBES and the bottom point

4. Results and Discussion

4.1. Experimental Data Design

Based on theoretical algorithms, we built a data model in Matlab/Simulink describing a model of the

movement and state of the system in actual operation to check the reliability of the algorithm. Assuming that the depth at the bottom of the lake is a sinusoid of amplitude and frequency, the device runs over the water in a straight line. Thus, the GPS data, after being separated from the packet according to the NMEA protocol, is a set of equally spaced points forming a straight trajectory.

The depth sensor data varies depending on the sinusoidal lake bottom as assumed. Finally, to simulate water surface waves, the white noise function is applied. Thus, the IMU data has been designed. However, the sampling frequency of each device can vary significantly based on the manufacturer's specifications. We choose the frequencies of GPS, IMU, and SBES, respectively, as 1 Hz, 100 Hz, and 5 Hz. The boat will run at a speed of 1 m/s. Finally, Fig. 6 can visualize the design data of the system.

GPS error is 0.02 m for GPS using RTK technology and 0.5 m for standard GPS. The SBES sensor has a resolution of 0.01 m at depths less than 10 m. We create examples incorporating the influence of instrument errors and compare the findings in each situation. Table 1 compares the relative position characteristics of GPS, IMU, and SBES.

Table 1. Relative position parameters between GPS, IMU and SBES

Level arm	Value
l_{gps}^{imu}	$[-0.2 \ -1 \ 0.3]$
l_{sbes}^{imu}	$[-2 \ 2 \ -1.3]$
R_{sbes}^{imu}	$[0 \ 0 \ 0]$

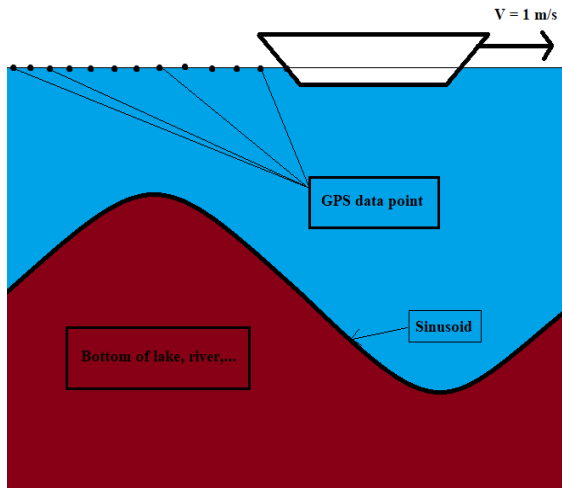


Fig. 6. Overview of the systems designed data

4.2. Analysis of the Results

After simulation using Matlab/Simulink, we get the results of error over time for each case, as shown in Fig. 7. It is clear to notice that the error of depth when utilizing the RTK measuring method most of the time

is below 0.5 m. Conventional measurement methods generate errors that generally exceeded 0.5 m. Furthermore, after including a more accurate depth sensor, the final result has improved. In order to more easily evaluate the error of the examples, we merge the cases on the same chart to appear like Fig. 8. Notice that the graph illustrates the erroneous case where the GPS error is 0.5 m larger than that of the GPS. The GPS error case is 0.02 m. Similarly to the depth sensor situation, where the device error is 0.25 m, the error graph is bigger when the device error is 0.01 m. In summary, through the error graph, the accuracy of the post calculation depth has been increased by enhancing the accuracy of the input devices. To appropriately examine the improvement of error, the average value of the error of the cases is shown in Table 2. Specifically, when employing RTK GPS, the technique produces a depth inaccuracy of up to 30.38 percent. When combined with the depth sensor's excellent accuracy, the error is reduced by 38.4 percent. So, when using high-precision input devices, the outcomes are greatly improved.

Table 2. Average depth error

Error parameter(m)	Average error(m)
<i>GPS error: 0.5</i>	<i>0.28847</i>
<i>GPS error: 0.02</i>	<i>0.200823</i>
<i>GPS error: 0.5 – SBES error: 0.25</i>	<i>0.251537</i>
<i>GPS error: 0.5 – SBES error: 0.25</i>	<i>0.154931</i>

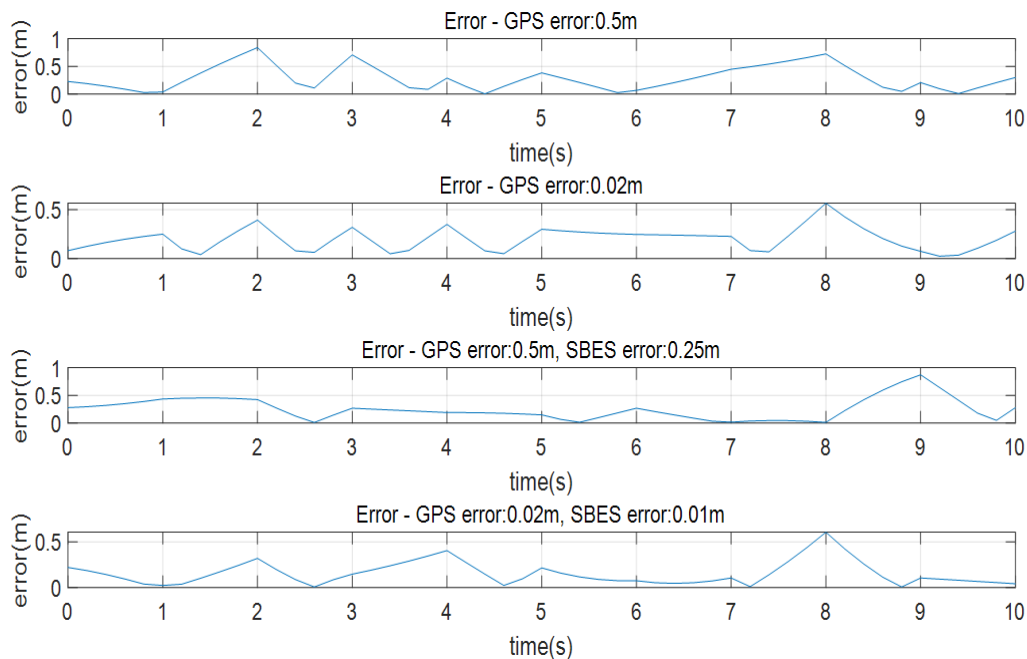


Fig. 7. Depth error of cases

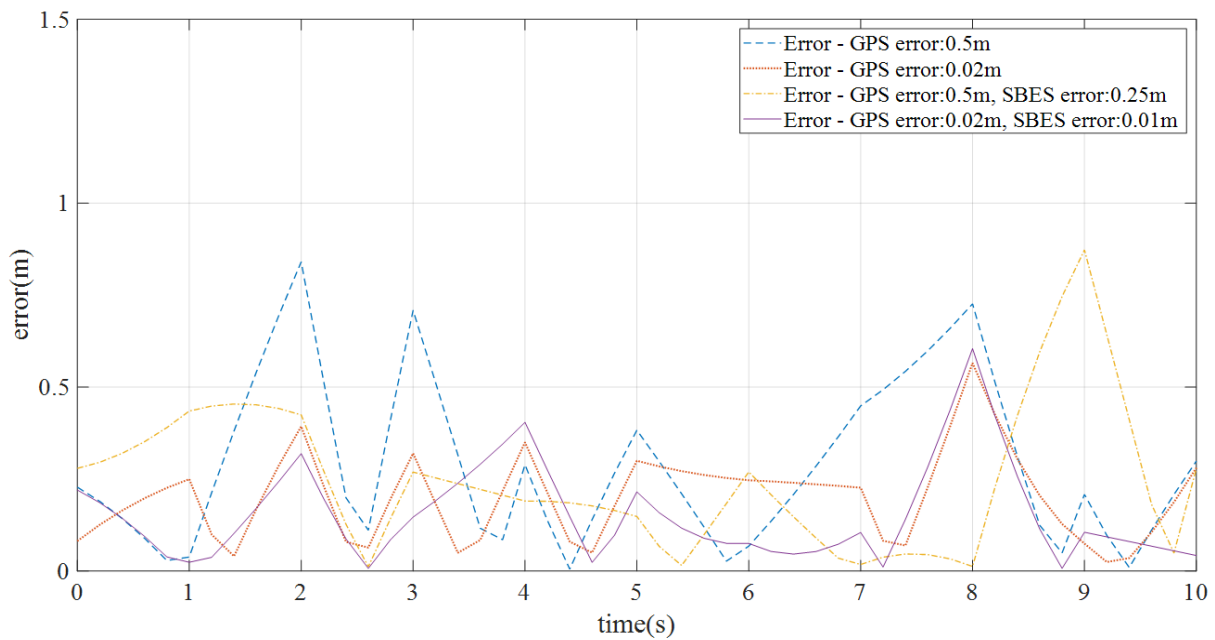


Fig. 8. Compare the errors in depth

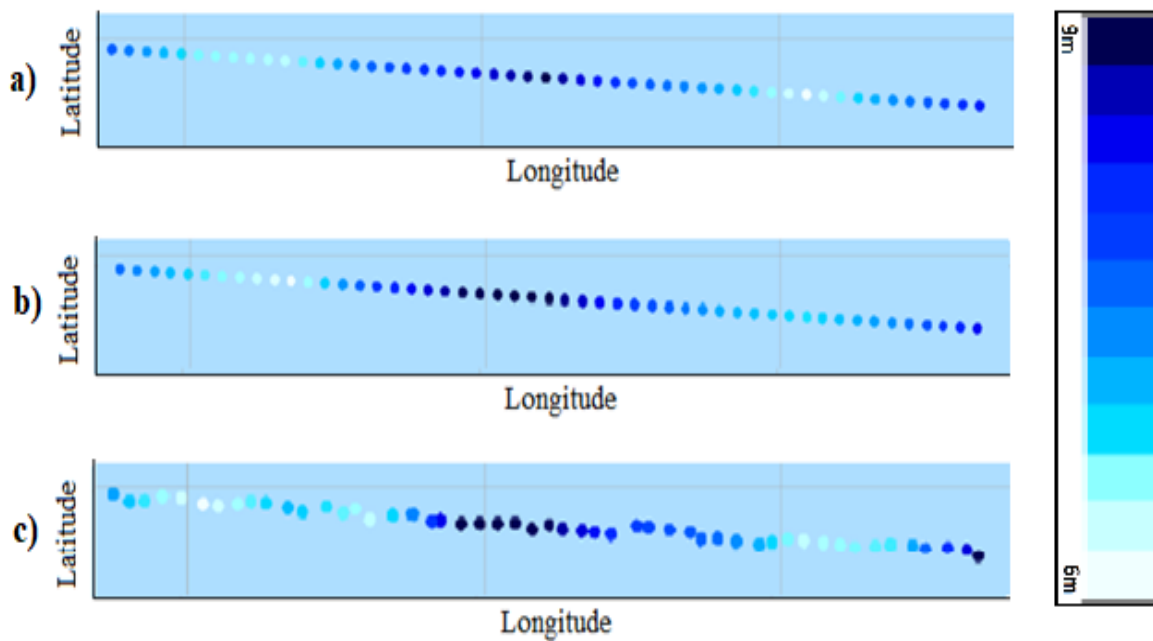


Fig. 9. Depth map by cases. (a) Real depth map. (b) Depth map with error improvement. (c) Depth map with large error device

After improving the accuracy of the depth, it is essential to construct a digital depth map of the survey region. Therefore, enhancing the position accuracy of the depth gauge points is important. Fig. 9 displays the depth map without an increase in input device accuracy and when it has improved. Fig. 9a is the exact depth map, Fig. 9b shows the depth map as input device accuracy improves. It is simple to observe. The placements of the measuring points and the depth are

comparable to reality, the mistake is extremely minimal, and it can be entirely utilized to generate a depth map. In contrast, with the standard measuring approach, the input data is not dependable, resulting in a depth map as illustrated in Fig. 9c. It can be seen that the depth measurement positions fully diverge from reality, as well as easily comprehend that the depth has a huge variance. Thus, with the standard measurement method, the depth survey map will be unreliable. In

short, the algorithm functioned and produced dependable results using better precision input devices.

5. Conclusion

This study proposes a method to determine the underwater topography by integrating a system including GPS RTK, IMU, and SBES. The collected data shows the coordinates and depth of points on the bottom surface, from which the depth map of the lake bed is generated. The test results show that the algorithm can be deployed when the device moves continuously while it is on the survey ship. This is one of the advantages of the system since it is capable of collecting data on the go. The test results also illustrate that the system is capable of synchronizing devices and calculating and correcting mistakes based on input data. This is achieved by creating a complete solution for computing software deployment, installation, and execution.

The method shows that by upgrading the RTK positioning technology, the quality of the depth sensor providing depth information is reduced by 38.4% compared with the traditional sensor. This is the premise for providing the right research roadmap for the ideal implementation of the GPS/IMU system combined with a single-beam echo depth sensor in the future, which will realize actual system integration and collect environmental data from rivers and lakes.

In the next stage, we will continue to develop an algorithm to reduce the influence of the environment (water waves, free obstacles such as aquatic species, etc.). In addition, we will also promote experimental surveys to collect results as a basis for improving the system and integrating the system into actual products such as boats and canoes to survey rivers and lakes in accordance with real conditions. Finally, our team will develop high precision products for various applications.

Acknowledgment

This research is funded by Hanoi University of Science and Technology (HUST) under grant number T2021-PC-041

References

- [1] E. Miguel, T. Hiroshi, M. Takahito, B. Lama, B. Austin, N Leonard, S. Tomoya, N. Mohammad, How to carry out bathymetric and elevation surveys on a tight budget:

basic surveying techniques for sustainability scientists, *International Journal of Sustainable Future for Human Security*, vol. 5, no. 2, pp. 86-91, Nov. 2017, <http://doi.org/10.24910/jsustain/5.2/8691>.

- [2] F. Bandini, D. Olesen, J. Jakobsen, C.M. Kittel, S. Wang, M. Garcia, P. Bauer-Gottwein, Technical note: Bathymetry observations of inland water bodies using a tethered single-beam sonar controlled by an unmanned aerial vehicle, *Hydrol. Earth Syst. Sci. Discuss*, Nov. 2017, <https://doi.org/10.5194/hess-2017-625>
- [3] A. Pirti, M. A. Yucel, K. Gumus, Testing real time kinematic GNSS (GPS and GPS/GLONASS) methods in obstructed and unobstructed sites, *Geodetski Vestnik*, vol. 57, no. 3, pp. 498-512, Sep. 2013. [Online]. Available: https://www.researchgate.net/publication/283252209_Testing_real_time_Kinematic_GNSS_GPS_and_GPS_GLONASS_methods_in_obstructed_and_unobstructed_sites
- [4] J. Zhao, X. Shang, H. Zhang, Reconstructing seabed topography from side-scan sonar images with self-constraint, *Remote Sens.*, vol. 10, no. 2, Jan. 2018, <https://doi.org/10.3390/rs10020201>.
- [5] R. Hare, Depth and position error budgets for multibeam echosounding, IHR, Monaco, Sep. 1995. [Online]. Available: <https://journals.lib.unb.ca/index.php/ihr/article/viewFile/23178/26953>
- [6] E. P. Larry, W. J. Lillycrop, C. J. Klein, R. C. P. Ives and S. P. Orlando, Use of lidar technology for collecting shallow water bathymetry of Florida Bay, *Journal of Coastal Research, Coastal Education & Research Foundation, Inc*, vol. 13, no. 4, pp. 1173-1180, 1997. [Online]. Available: <https://journals.flvc.org/jcr/article/view/80361/77602>
- [7] S. P. Drake, Converting GPS Coordinates ($\phi\lambda$) to Navigation Coordinates (ENU), DSTO Electronics and Surveillance Research Laboratory, Edinburgh, South Australia, Australia, April. 2002. [Online]. Available: https://www.researchgate.net/publication/27253833_Converting_GPS_coordinates_phi_lambda_h_to_navigation_coordinates_ENU
- [8] M. Dix, A. Abd-Elrahman, B. Dewitt and L. Nash Jr, Accuracy evaluation of terrestrial LIDAR and multibeam sonar systems mounted on a survey vessel, *J. Surv. Eng.*, vol. 138, no. 4, pp. 203-213, Nov. 2012, [https://doi.org/10.1061/\(ASCE\)SU.1943-5428.0000075](https://doi.org/10.1061/(ASCE)SU.1943-5428.0000075)